

(CMA) and a Comparator are used to test both subcircuits. In the first phase ($Test_sub-CUT_R$ is “high” and $Test_sub-CUT_L$ is “low”) the background current I_{BL} of the sub- CUT_L , at the REF port of the CMA, is mirrored properly to its $CMPS$ port and thus to the sensing node V_{Gnd_R} of the sub- CUT_R . This way a compensation current $I_{CMP_R} = \beta_L I_{BL} = I_{BR}$ is generated that sinks the background current of sub- CUT_R . As a result, in the fault free case, the voltage on node V_{Gnd_R} drops below the reference voltage V_{REF} of the comparator. However, in the presence of a fault in sub- CUT_R the additional defective current raises the voltage at the sensing node V_{Gnd_R} above the V_{REF} voltage and the fault is detected. The phase ends turning T_ENB back to “high”. In a similar way during the second phase ($Test_sub-CUT_R$ is “high” and $Test_sub-CUT_L$ is “low”) the compensation current $I_{CMP_L} = \beta_R I_{BR} = I_{BL}$ at the sensing node V_{Gnd_L} is generated in order to test sub- CUT_L . Note that β_L and β_R can take values lower than unity.

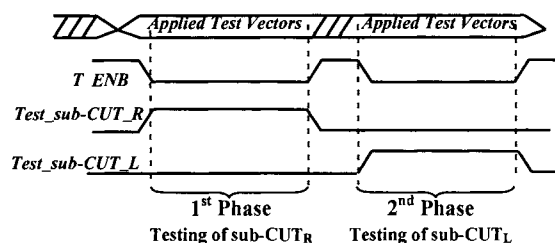


Figure 2. I_{DDQ} testing signals' waveforms

In Fig. 3 an effective ground supply partitioning technique is illustrated (similarly a V_{DD} supply partitioning scheme can be used) that provides equivalent dependence of both compensation currents on process and temperature variations by interdigitating inside the CUT two independent ground rails.

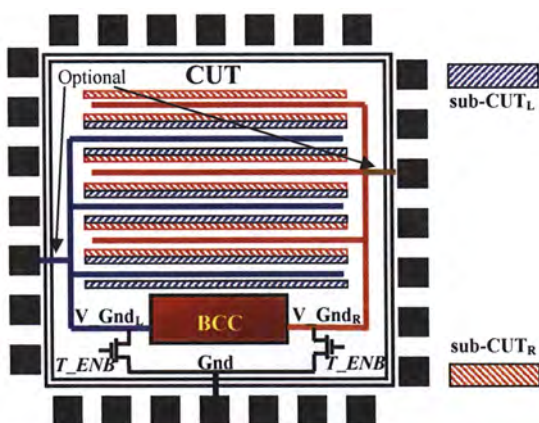


Figure 3. Possible supply partition technique (power rail)

However, the background current also depends on the applied test vector. In order to take into account this dependence a Programmable Current Mirror/Amplifier (PCMA) has been adopted for the implementation of the BCC circuit, that is a CMA with programmable current

gain β . In that case simulations should be carried out in order to determine the required gain of the PCMA for each test vector of the test set applied to the CUT. This approach is applicable since the cardinality of an I_{DDQ} test set is very small [5]. Moreover, selecting suitably the proper test vectors, based on static power analysis [6-7], we can further reduce the background current variations from test vector to test vector. Then we can group together the test vectors for which the corresponding background currents present neighboring values keeping the size of the PCMA small. Possible differences between the simulated and the actual, in the field, background currents of the CUT do not invalidate the method since these variations affect in the same way both background currents.

3. I_{DDQ} TEST CHIP: EXPERIMENTAL RESULTS

3.1. The Demonstration circuit

In order to validate the proposed I_{DDQ} testing technique a demonstration circuit has been designed and fabricated in the standard $0.18\mu\text{m}$ CMOS technology of ST-Microelectronics ($V_{DD}=1.8\text{V}$). The demonstrator consists of a digital circuit, a PCMA circuit and a comparator that is used to discriminate defect free from defective cases. In addition a faulty cell constructed of two inverters with a $1\text{K}\Omega$ resistance short circuit between their outputs is present. The faulty cell shares the same virtual ground (V_{Gnd}) with one subcircuit and can be properly activated by a $Fault_Enable$ signal in order to insert a bridging fault in the circuit under test. However, it is possible to connect externally, between V_{DD} and V_{Gnd} nodes, any desired resistance value. The microphotograph of the demonstrator is shown in Fig. 4.

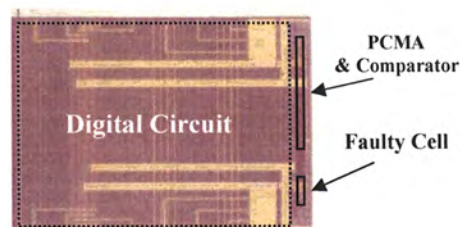


Figure 4. I_{DDQ} test chip microphotograph

A. The digital circuit: The digital circuit is the CUT. It is constructed of 10800 two input NAND and 10800 two input NOR gates. The circuit is partitioned into two subcircuits according to the ground supply partitioning technique of Fig 3. Each subcircuit contains half of the total circuit gates. For each subcircuit all its NAND gates are driven by a pair of signals and all its NOR gates are driven by another pair of signals. These eight signals in total are exploited to control the I_B of each subcircuit. This current ranges from about 100nA up to $10\mu\text{A}$ for all input combinations (256 combinations) in all process corners.

Although the size of the digital circuit is small to provide large background currents, this magnitude is not important in the validation of the proposed technique.

What is essential is the ability of this method to discriminate defect free from defective circuits when the background currents and the defective currents (to be detected) are comparable and a single voltage threshold is used.

B. The PCMA circuit: The design of the PCMA is shown in Fig. 5 and is based on the Wilson current mirror topology that has been selected due to its high output resistance [8]. It consists of six branches, three at the side of the reference port (*REF*) and three at the side of the compensation current generation port (*CMPS*). These mirrors act as current sinks at the virtual ground of the sub-CUT_{RL} under test in order to sink its background current $I_{B(RL)}$. The reference current at the *REF* port of the PCMA is mirrored to its *CMPS* port and thus to the sensing node. Six select signals (SEL_1 - SEL_6), one for each branch, are exploited to provide the programmability of the current mirror. These signals drive the select transistors MS_1 - MS_6 and the corresponding full CMOS pass gates providing the ability to synthesize the proper compensation current for each test vector that is applied to the CUT.

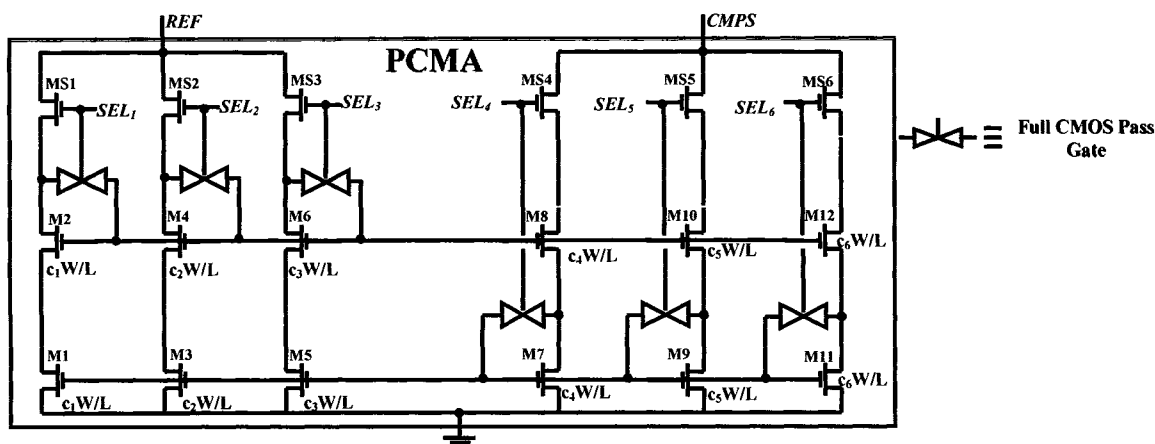


Figure 5. The used PCMA circuit

The widths of PCMA transistors used in the demonstration circuit are: i) for M_1 , M_2 and MS_1 $W=20\mu\text{m}$, ii) for M_3 , M_4 and MS_2 $W=30\mu\text{m}$, iii) for M_5 , M_6 and MS_3 $W=100\mu\text{m}$, iv) for M_7 , M_8 and MS_4 $W=50\mu\text{m}$, v) for M_9 , M_{10} and MS_5 $W=100\mu\text{m}$ and vi) for M_{11} , M_{12} and MS_6 $W=200\mu\text{m}$. These widths have been selected after electrical simulations for every input combination of the digital circuit, in every process corner of the used technology, and for temperatures from 25 to 85 °C, to generate all the required compensation currents. The length L of all transistors is 0.5 μm . For the needs of a complete I_{DDQ} testing of the CUT, considering all input combinations in all possible process corners, only 10 states are required from a total of 49 PCMA programmable states.

C. The Comparator: The comparator is a simple differential amplifier that has been selected for its very high input resistance in order to avoid disturbing the compensation mechanism of the PCMA. One of the comparator's inputs is connected to the *CMPS* port of the

PCMA and the other to a reference voltage $V_{REF}=0.9V$ (see Fig. 1). The comparator has been designed so that its digital (fault indication) output *Fail/Pass* provides, during I_{DDQ} testing, a "high" response in case that a fault is present and a "low" response in the fault free case.

The required silicon area for the PCMA circuit and the comparator is only the 2.42% of the digital circuit under test. However, it is not necessary for the proposed technique any of these two circuits to be embedded with the CUT. This alternative approach may provide a higher flexibility in the design of these circuits. The only requirement is the proper partitioning of the CUT.

3.2. Experimental Results

According to the proposed I_{DDQ} testing technique, for every subcircuit and for every combination (test vector) at the inputs of the digital circuit a distinct activation vector $\langle SEL_1$ - $SEL_6 \rangle$ for the select signals has been determined through simulations in all process corners. This set of activation vectors has been used during the evaluation of the fabricated I_{DDQ} test chip (see Table I).

Table I - Test vector distribution per activation vector

Activation Vector $\langle SEL_1$ - $SEL_6 \rangle$	Current Mirror Amplification Factor (β)	Number of Test Vectors
$\langle 100 - 010 \rangle$	200/20	2
$\langle 100 - 110 \rangle$	300/20	6
$\langle 010 - 100 \rangle$	100/30	10
$\langle 010 - 010 \rangle$	200/30	46
$\langle 010 - 110 \rangle$	300/30	2
$\langle 001 - 001 \rangle$	50/100	24
$\langle 001 - 100 \rangle$	100/100	129
$\langle 001 - 101 \rangle$	150/100	1
$\langle 001 - 010 \rangle$	200/100	32
$\langle 001 - 110 \rangle$	300/100	4
Total Test Vectors:		256

The evaluation procedure was as follows:

- initially, the input vector is applied to the digital circuit while the virtual grounds ($V_{Gnd_{L/R}}$) are

grounded (T_ENB is “high”) and the PCMA and the faulty cell are inactive (fault free case – PCMA inactive);

- b) then, the T_ENB is set to “low” and the I_{DDQ} test result is observed at the *Fail/Pass* port;
- c) next, the T_ENB is set to “high” and the PCMA is activated applying the corresponding, predetermined activation vector (fault free case – PCMA active);
- d) subsequently, the T_ENB is turned to “low” and the *Fail/Pass* signal is read,
- e) next, the T_ENB is turned to “high” and the faulty cell is also activated (faulty case – PCMA active),
- f) finally, the T_ENB is set to “low” and the *Fail/Pass* signal is observed.

This procedure has been followed for every possible input vector and the experimental results have shown that there is never an erroneous fault indication in the fault free case when the PCMA is active and that there is always a fault detection indication when a fault is present and the PCMA is active. This means that the proposed technique fulfills I_{DDQ} testing requirements without any loss either in the yield or the fault coverage. However, as it is illustrated in the logic analyzer view of Fig. 6 there were fault free cases, with the PCMA inactive (procedure steps a and b), where the result was an erroneous fault indication, which means that without the proposed technique these cases will lead to yield loss when a single discrimination threshold (V_{REF}) is used.

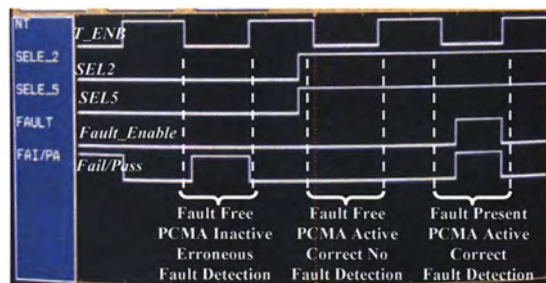


Figure 6. Experimental results from the fabricated chip

In order to characterize the I_{DDQ} test circuit and determine its resolution, external short circuit resistances with values up to $20M\Omega$ ($I_{DEF}=90nA$) have been used. The measurements show that this circuit is capable to detect defective currents down to 3% of the circuit background current. Since the majority of defective resistances in a chip is up to 500Ω [9], then setting the desirable range of detectable defective resistances up to this value, which corresponds to a defective current up to 3.6mA (considering $V_{DD}=1.8V$), it is implied that with a 3% resolution the proposed design approach can be applied to circuits with background currents up to 0.12A. This is a very attractive result since it covers a wide range

of circuit designs in this technology node. However, for higher background currents more partitions can be used.

4. CONCLUSIONS

In this work early experimental results on a new I_{DDQ} testing technique are presented. According to this technique, during I_{DDQ} testing, the background current at the sensing node of the CUT is compensated taking into account possible manufacturing process and temperature variations as well as the dependence of the background current on the applied test vector. This way any excessive defective current can be detected applying well known, simple, fast and high resolution sensing techniques using a single discrimination threshold. The adoption of this method is a promising solution to extend the viability of I_{DDQ} testing in future nanometer technologies.

5. ACKNOWLEDGMENT

The authors would like to thank Guillaume Prenat and Salvador Mir from TIMA Laboratory, Grenoble, France, for their suggestions and their support in the test chip fabrication.

6. REFERENCES

- [1] S. Sabade and D. Walker, “ I_{DDQ} Test: Will It Survive the DSM Challenge?”, IEEE Design and Test of Computers, vol. 19, no. 5, pp. 8-16, 2002.
- [2] R.R. Montanes and J. Figueras, “Estimation of the Defective I_{DDQ} Caused by Shorts in Deep Submicron CMOS ICs”, Design Automation and Test in Europe (DATE), pp. 490-494, 1998.
- [3] S. Borkar, “Design Challenges of Technology Scaling”, IEEE Micro, pp. 23-29, July-August, 1999.
- [4] Y. Tsiatouhas, Th.Haniotakis, D. Nikolos and A. Arapoyianni, “Extending the Viability of I_{DDQ} Testing in the Deep Submicron Era”, IEEE International Symposium on Quality Electronic Design (ISQED), pp. 100-105, 2002.
- [5] E.Isern and J. Figueras, “Test Generation with High Coverages for Quiescent Current Test of Bridging Faults in Combinational Circuits”, International Test Conference (ITC), pp. 73-82, 1993.
- [6] P.C. Maxwell and J.R. Rearick, “A Simulation-Based Method for Estimating Defect-Free I_{DDQ} ”, IEEE International I_{DDQ} Testing Workshop, pp.80-84, 1997.
- [7] Z. Chen, M. Johnson, L. Wei and K. Roy, “Estimation of Standby Leakage Power in CMOS Circuits Considering Accurate Modeling of Transistor Stacks”, International Symposium on Low Power Electronics and Design, pp. 239-244, 1998.
- [8] P. Gray, P. Hurst, S. Lewis and R. Meyer, “Analysis and Design of Analog Integrated Circuits”, Wiley, 2001.
- [9] J.J. Tang, K.J. Lee and B.D. Liu, “A Practical Current Sensing Technique for I_{DDQ} Testing”, IEEE Transactions on VLSI Systems, vol. 3, no. 2, pp. 302-310, 1995.